

Star formation efficiency in Centaurus A.

Hao-Ren Jheng

National Central University

August 28, 2015

Abstract

Based on the CO(2-1) observations from ALMA and infrared data using the imaged taken by Spitzer Space Telescope, I calculated surface densities of molecular gas and star formation rate (SFR). Knowing the column density of molecular clouds and SFRs of the selected regions, I also checked the Schmidt-Kennicutt law. The result shows the power law index is about 0.63, which is smaller than typical value.

1 Introduction

The Centaurus A was first discovered by the Scottish astronomer James Dunlop from Parramatta observatory in Australia on August 4, 1826. When observed in optical wavelengths, it looks like an elliptical galaxy with a dust band. Because of their poor dust and gas contents, ellipticals typically don't have dust bands, and their SFRs are relative low. However, several researches showed that Centaurus A is a starburst galaxy, with more than 100 regions of star formation identified in the galaxy's disk. The peculiar characters of this galaxy interests me to do the study.

In 1959, Maarten Schmidt introduced a simple gas-density power law, which described the relation between the observable surface densities of gas and star formation. It can be written as

$$\sum_{SFR} = A(\sum_{gas})^N$$

The Schmidt law has been tested in many star forming galaxies, with the power index N within the range $1 - 2$. After about 40 years, Robert C. Kennicutt Jr. obtained the result with the index $N = 1.4 \pm 0.15$ (1998)

$$\sum_{SFR} = (2.5 \pm 0.7) \times 10^{-4} \left(\frac{\sum_{gas}}{1M_{\odot}/pc^2} \right)^{1.4 \pm 0.15} M_{\odot}/(yr \cdot kpc^2)$$

In order to get the power law of Centaurus A, I need to check the surface density of molecular gas and SFR.

From previous study, the dust emission at 8.0 micron can be used as a star formation indicator (e.g., Wu et al. 2005). I calculated the dust emission from the 3.6 μ m and 8.0 μ m fluxes

$$flux_{8.0\mu m(dust)}[MJy/sr] = flux_{8.0\mu m} - \eta \cdot flux_{3.6\mu m}$$

Where $\eta = 0.232$ (Leitherer et al. 1999; Helou et al. 2004). The images I used are from Infrared Array Camera (IRAC) on the Spitzer Space Telescope. The surface density of star formation rate can be derived from 8.0 μm dust emission (Wu et al. 2005)

$$\frac{\Sigma_{SFR}}{1 [M_{\odot}/yr]} = \frac{\nu \cdot L_{8.0\mu m(dust)}}{1.57 \times 10^9 L_{\odot}}$$

where $L_{8.0\mu m(dust)}$ is 8.0 μm dust luminosity.

CO is a widely used molecular gas tracer. We can use the CO flux with the CO-to-H₂ conversion factor X to estimate the mass of the molecular gas. The factor $X = 3.0 \times 10^{20} [(K \cdot km/s)^{-1}]$ (e.g., Solomon et al. 1987; Young&Scoville, 1991)

$$\left(\frac{M_{H_2}}{1 M_{\odot}} \right) = 1.2 \times 10^{-4} \times \left(\frac{S_{CO}}{1 [Jy \cdot km/s]} \right) \times \left(\frac{D}{1 [Mpc]} \right)^2$$

$$M_{gas} [M_{\odot}] = 1.36 M_{H_2}$$

(Kazushi Sakamoto & Sachiko Okumura, 1995). The equations above are for CO(1-0) transition, while the image I used is CO(2-1) observation. I should do some assumptions to make calculation reasonable. I assume that the CO(2-1) gas is dense enough that we can treat it as optically thick matter, and the gas is in thermal equilibrium state. Because gas is in thermal equilibrium, the brightness temperature is constant. The Planck function in frequency form is

$$I_{\nu}(T) = \frac{2h \frac{\nu^3}{c^2}}{e^{\frac{h\nu}{kT}} - 1} \left[\frac{W}{sr \cdot m^2 \cdot Hz} \right]$$

where ν is frequency, T is temperature, c is the speed of light, h is the Planck constant, k is the Boltzmann constant. In radio range, $h\nu \ll kT$. The Planck can be written as

$$I_{\nu}(T) = 2 \frac{\nu^2}{c^2} kT$$

so

$$T = \frac{I_{\nu} \cdot c^2}{2k\nu^2}$$

Since the temperature is constant,

$$\frac{I_{\nu}}{\nu^2} = const.$$

Hence, we can get the ratio of CO(2-1) to CO(1-0)

$$\frac{I_{CO(2-1)}}{I_{CO(1-0)}} = \frac{\nu_{CO(2-1)}^2}{\nu_{CO(1-0)}^2}$$

The frequency of CO(2-1) emission is about 230.538 GHz, while that of CO(1-0) is about 115.2712

GHz. As a result, a factor of 0.25 should be added to the formula calculating the mass of the molecular gas.

2 Method

Since the resolutions and regions scanned over by antennas of ALMA or Spitzer telescope of the three images are different, I need to do the “regrid”. I used CASA software to do this task. I regridded the two Spitzer images into the CO integrated intensity map form. Besides, in the original images, there are some regions that do not carry any information. For some reasons, the system didn't record value in these areas. To fix this deficiency, I used IDL (Interactive Data Language) to read the three images, and then substituted the values of these regions by 0. Next, I applied the equations mentioned before to calculate the $8.0\mu\text{m}$ dust flux, and produce an image. I used DS9 to read the $8.0\mu\text{m}$ dust image, add the contour of CO moment 0 map, choose the regions, and finally save the image coordinates of these regions in a text file. There are total for 209 regions, 76 for high SFR and 133 for low SFR. After these works, I again used IDL to read the coordinates information and calculate the surface densities of SFRs and molecular cloud.

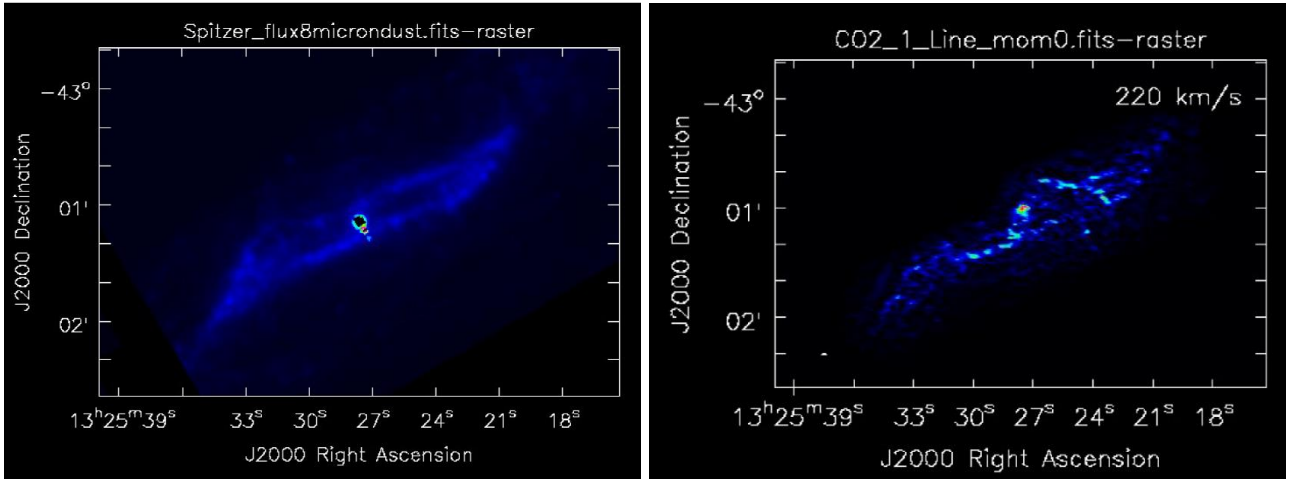


Figure 1: The left one is the $8.0\mu\text{m}$ dust image of Centaurus A. The right one is the CO(2-1) integrated intensity (moment 0) map. The beam size of these two images is $2''.93 \times 0''.84$.

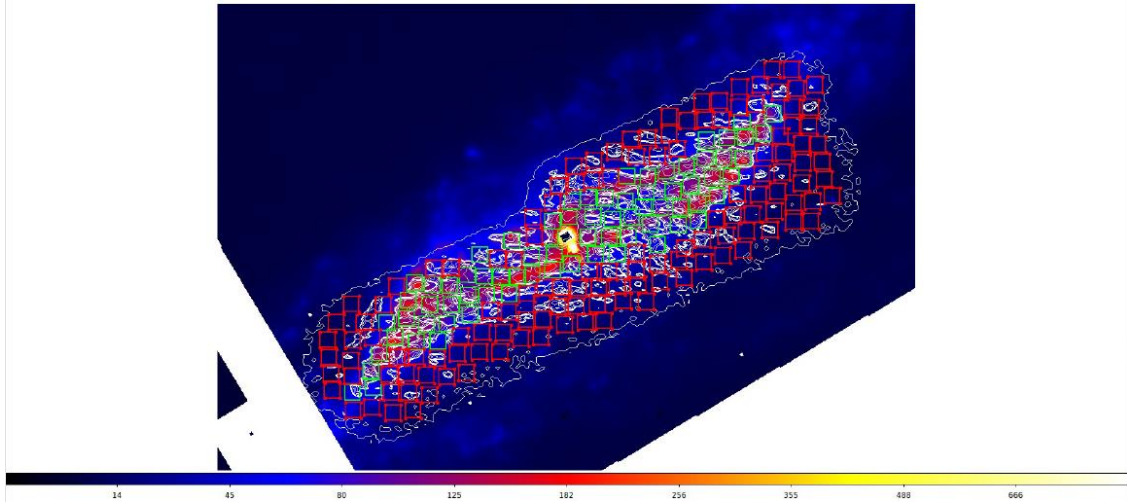
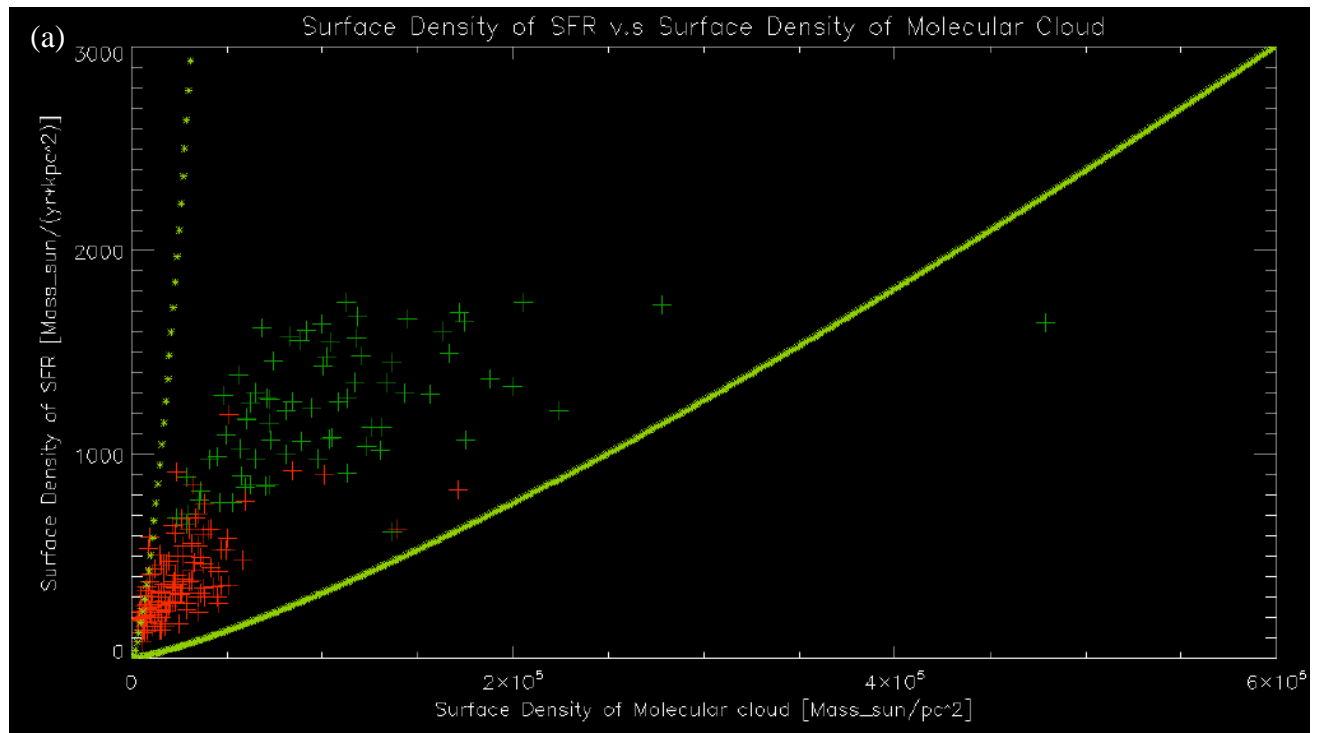


Figure 2: This figure shows regions I selected to calculate the surface densities of SFRs and molecular gas. The color image is the 8.0 μ m dust image. The contour is the CO(2-1) integrated intensity map. The green regions are high SFR places, while those in red are relatively low SFR places.

3 Results and discussion

Base on the equations in Introduction, I wrote an IDL program for calculating. I show the results in the following figures.



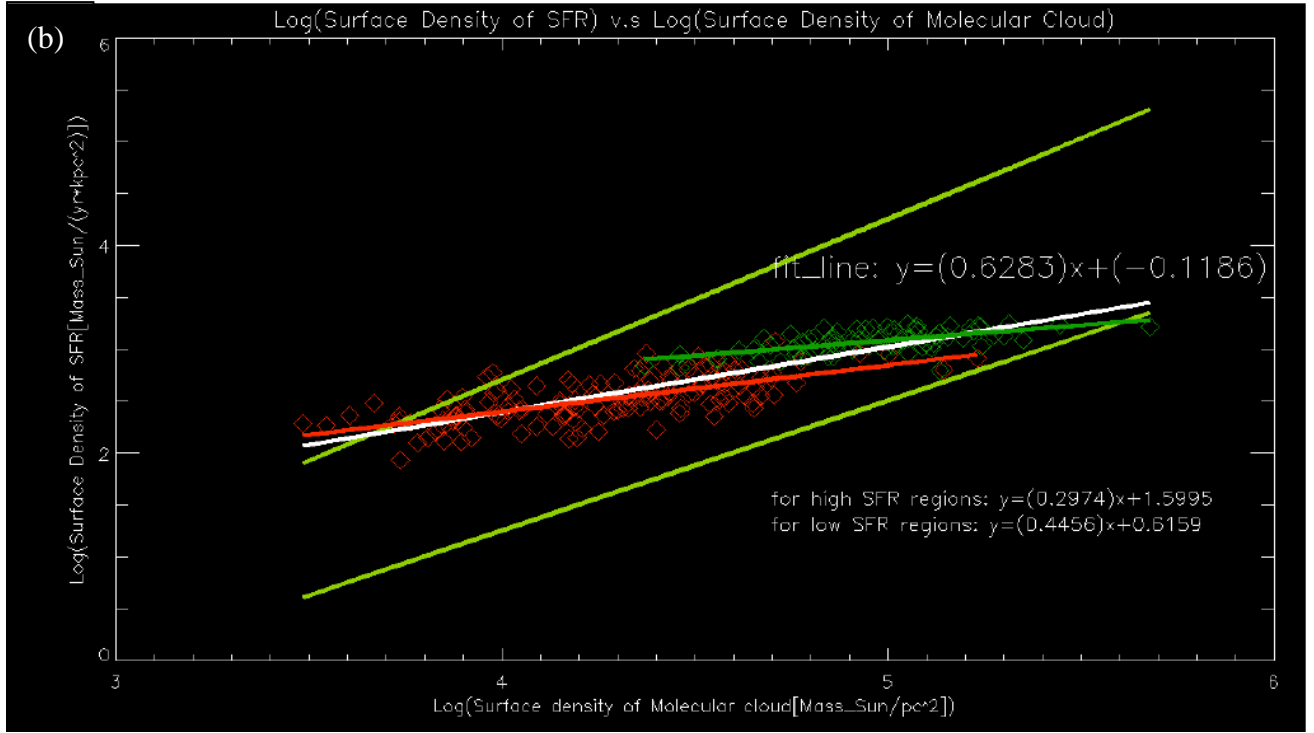


Figure 3: (a) The surface density of SFRs versus the surface density of molecular cloud. (b) After taking logarithm. The red and green regions are corresponding to the regions shown in Fig. 2. The light green line are the upper and lower limit of SFR according to the relation obtained by Kennicutt. The white line in (b) is the least square fitting line, with the slope of 0.6283, which is smaller than typical power law index value.

Figure 3(a) shows the surface density of SFRs versus the surface density of molecular cloud, and 3(b) shows the data after taking logarithm. The light green line are the upper and lower limit of SFR according to the relation obtained by Kennicutt. The least square method is used to fit the data points. The power law index of the fitting line is 0.6283, which is smaller than typical value.

When deriving the ratio of CO(2-1) to CO(1-0), I assume that CO(2-1) is optically thick. That is, the density of CO(2-1) reaches the critical density. However, the real situation might not be similar as my assumptions. If the densities of the molecular clouds are lower than the critical density of CO(2-1), it would cause the number of molecules excited from lower energy level to higher energy level is less than those drop from higher energy level to lower energy level. In other words, this would not be a thermal equilibrium state. For the situation that the gas densities are smaller than the critical density, observations will pick out only high-density peaks (e.g., Mark R. Krumholz & Todd A. Thompson, 2007). As a result, the less the surface density is, the more I underestimate its value. If I take this in to consideration, the slope of the fit line would be larger. Careful studies and observations are still needed for the exact reasons of the flatter slope.

4 Conclusions

In my study, I obtained the Schmidt-Kennicutt law of Centaurus A. The power law index is 0.6283, which is smaller than widely accepted value 1.4 ± 0.15 . My guess is that the low density of CO(2-1) contributes to the smaller power law index. More detail studies are still needed to check the correctness of my results and speculations.

References

- Helou, G., Roussel, H., Appleton, P., et al. 2004, ApJS, 154, 253
- Kazushi Sakamoto, Sachiko Okumura, 1995, ApJ, 110, 5
- Kennicutt, R. C. 1998, ApJ, 498, 541
- Krumholz, M. R., & Thompson, T. A. 2007, ApJ, 669, 289
- Leitherer, C., Schaerer, D., Goldader, J. D., et al. 1999, ApJS, 123, 3
- Mengchun Tsai, Chorng-Yuan Hwang, et al. 2012, ApJ, 746, 129
- Schmidt, M. 1959, ApJ, 129, 243
- Solomon, P. M., Rivolo, A. R., Barrett, J., & Yahil, A. 1987, ApJ, 319, 730
- Wu, H., Cao, C., Hao, C.-N., et al. 2005, ApJ, 632, L79
- Young, J. S., & Scoville, N. Z. 1991, ARA&A, 29, 581